Absolute vs. Relative Error Characterization of Electromagnetic Tracking Accuracy

Mohammad Matinfar, Ganesh Narayanasamy, Luis Guitierrez,
Raymond Chan* and Ameet Jain*

Department of Interventional Guidance Technology
Philips Research North America, Briarcliff, NY, USA

ABSTRACT

Electromagnetic (EM) tracking systems are often used for real time navigation of medical tools in an Image Guided Therapy (IGT) system. They are specifically advantageous when the medical device requires tracking within the body of a patient where line of sight constraints prevent the use of conventional optical tracking. EM tracking systems are however very sensitive to electromagnetic field distortions. These distortions, arising from changes in the electromagnetic environment due to the presence of conductive ferromagnetic surgical tools or other medical equipment, limit the accuracy of EM tracking, in some cases potentially rendering tracking data unusable. We present a mapping method for the operating region over which EM tracking sensors are used, allowing for characterization of measurement errors, in turn providing physicians with visual feedback about measurement confidence or reliability of localization estimates.

In this instance, we employ a calibration phantom to assess distortion within the operating field of the EM tracker and to display in real time the distribution of measurement errors, as well as the location and extent of the field associated with minimal spatial distortion. The accuracy is assessed relative to successive measurements. Error is computed for a reference point and consecutive measurement errors are displayed relative to the reference in order to characterize the accuracy in near-real-time. In an initial set-up phase, the phantom geometry is calibrated by registering the data from a multitude of EM sensors in a non-ferromagnetic ("clean") EM environment. The registration results in the locations of sensors with respect to each other and defines the geometry of the sensors in the phantom. In a measurement phase, the position and orientation data from all sensors are compared with the known geometry of the sensor spacing, and localization errors (displacement and orientation) are computed. Based on error thresholds provided by the operator, the spatial distribution of localization errors are clustered and dynamically displayed as separate confidence zones within the operating region of the EM tracker space.

Keywords: Interventional guidance, electromagnetic tracking, calibration, performance characterization, localization and tracking technologies

1. INTRODUCTION

Many clinical procedures require the tracking of medical instrumentation within the patient's body. In these applications, optical tracking systems cannot be used because of line of sight (LOS) constraints typically encountered. EM tracking systems provide a viable alternative that does not suffer from LOS limitations. EM tracking systems perform relatively stably in electromagnetically "clean", non-ferromagnetic environments. However, significant spatial distortion can occur when there are sources of distortion near the field generator or sensor coils[1,2] e.g. an X-ray C-arm gantry, medical monitoring equipment generating EM interference, etc. Mean measurement errors have been reported to be several millimeters in position and several degrees in orientation.[3] Different protocols have been suggested to evaluate the accuracy of these systems in different clinical environments.[4,5]

Several researchers have investigated methods to model the measurement error and then compensate for it. They are mainly referred to in literature as methods for EM tracking calibration since they perform a one-time calibration pre-procedurally, followed by using an interpolation algorithm to correct for measurement distortions.

*Corresponding authors: Drs. R. Chan & A. Jain; ray.chan@philips.com; ameet.jain@philips.com; 1-914-434-4784

Medical Imaging 2010: Visualization, Image-Guided Procedures, and Modeling, edited by Kenneth H. Wong,
Michael I. Miga, Proc. of SPIE Vol. 7625, 762524 · © 2010 SPIE · CCC code: 1605-7422/10/$18 · doi: 10.1117/12.844326

Downloaded From: http://proceedings.spiedigitallibrary.org/ on 05/10/2013 Terms of Use: http://spiedl.org/terms

However, most of these methods have been studied within a static environment in which the source of distortion is constant, e.g. a conductive or ferromagnetic distortion in vicinity of the electromagnetic field or sensor coils. In practice, medical intervention suites are dynamically changing and operating instruments that produce EM distortions distortion actively move within the workspace of interest. These instruments have different sizes and different material composition and some instruments have significant distorting effects such as X-ray gantries, CT scanners, etc. These distortions vary with instrument positioning and create a dynamic environment where makes it almost impossible to predict the distortion error in great detail.

The main method for calibration of EM tracking systems is performed by registering data from an optical tracking system and the Aurora tracking system.[6] The result of registration with a calibration phantom is used to compute an interpolation function based on the assumption that the geometric errors associated with different sensor orientations can be calibrated independently. Then, using a spherical interpolation triangle, the error is computed and corrected for in subsequent measurements. This method is further elaborated where a Bernstein polynomial model of measurement error has been developed.[7] Selecting a set of basis orientation vectors, the resulting least squares problem is solved by estimating the weighting coefficients associated with the unknown Bernstein polynomials. The main issue in these methods is the high dimensionality of the error space and sparsity of calibration measurement points, making this a classic ill-posed inverse problem. For example, for a 3rd order Bernstein polynomial and a 6 vector basis, the least squares inverse problem requires solving for 2304 unknown coefficients.

2. METHODS AND MATERIALS

2.1 Data Collection

The experimental setup is composed of three main components: a three-axis positioning robot (Velmex Inc., Bloomfield, NY), an NDI Aurora electromagnetic tracking system (Northern Digital Inc., Waterloo, Canada) and a custom calibration phantom geometry containing 6 EM sensors. The robot provides three orthogonal degrees of motion that are used to position the phantom in space. Each axis of the positioning robot uses an independent stepper motor coupled to a lead screw which together provides submillimeter resolution and accuracy.

The calibration geometry consists of a cubical phantom that accommodates 6 sensors, with 2 sensors each of the X, Y and Z axes under interrogation. The sensors are located at a known and fixed distance relative to one another to avoid mutual interference. In an initial configuration phase, this phantom is calibrated in a distortion-free environment. By moving the phantom in a clean EMenvironment, data are collected for the 2 sensors in each axis. A rigid transformation is found between these two sets of data using a subset of sample locations. The translation vector of this transformation provides the distance between the two sensors. The same procedure is applied to other sensors and the distances between sensors for all axes are found. Figure 1 depicts one embodiment of the phantom. .

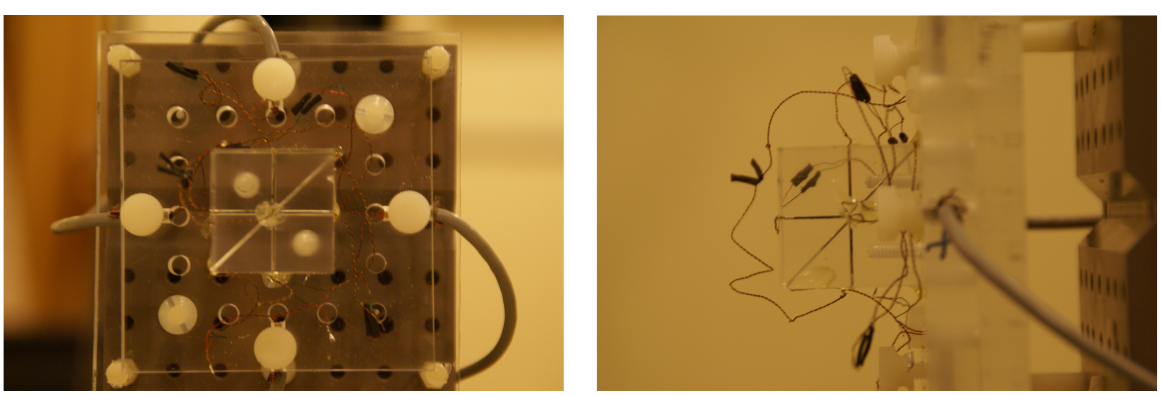

Figure 1. Calibration phantom with two 5-DOF sensors in each axis spaced at a fixed 10mm from each other.

Downloaded From: http://proceedings.spiedigitallibrary.org/ on 05/10/2013 Terms of Use: http://spiedl.org/terms

Figure 2. Experimental setup in an interventional X-ray suite showing (a) Aurora field generator, (b) positioning system, (c) phantom mounted on a non-metallic extension arm in the present of an interventional imaging system.

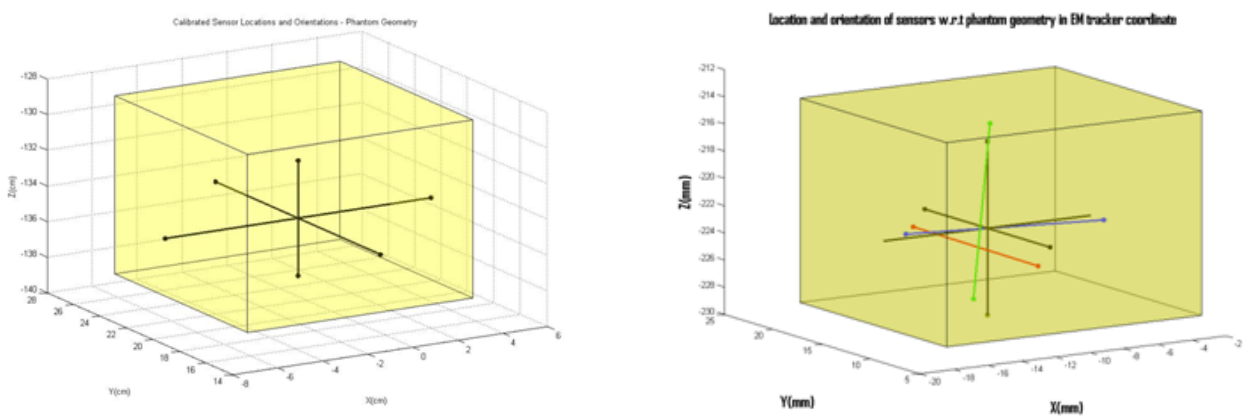

(a) (b)

Figure 3. (a) Calibrated sensor locations and orientations - phantom geometry. (b) Location and orientation of sensors w.r.t phantom geometry in an interventional X-ray environment.

For each sampled point, the positioning system moved the phantom to each location, pausing at each sample point in space to allow for position/orientation measurements to be collected from the Aurora for all 6 sensors. The reported position at each location for each sensor was computed as an average of 20 measurements from the Aurora tracking system. The robotic positioning system provided the "ground truth" for expected positions used for reference comparison, whereas the Aurora dataset contained the actual measurements from EM sensing Since the robotic positioning system and the Aurora EM system operate in different coordinate spaces, the Aurora position data was registered to the positioning system data using a rigid body transformation minimizing the least squares L2-norm between the subset of position sample points used for registration. The experimental setup in the interventional X-ray suite is shown in Figure 2.

Figure 3(a) shows the geometry of the sensors in the cubical phantom which resulted from calibration. Data were collected in different environments to observe the behavior of the Aurora measurements as a function of surroundings. These measurements were used to map the error field, helping us to understand the operating characteristics of the Aurora tracking system. Figure 3 (b) illustrates one of the EM measurements obtained when the location and orientation of sensors are compared with the calibrated ones. Data in this figure is collected in the presence of an X-ray system, which introduces ferromagnetic distortion into the EM measurements. Clearly there is considerable error visible in both sensor orientation and location.

Downloaded From: http://proceedings.spiedigitallibrary.org/ on 05/10/2013 Terms of Use: http://spiedl.org/terms

2.2 NURBS-Kernel Error Compensation

An interpolation function that is often used in computer-aided-design to precisely define curves in complex shapes is the non-uniform rational B-spline (NURBS).[8] The idea of NURBS-based error compensation is to find a vector of control points that can sufficiently model the error and then compensate for it in an unwarping correction step. We assume that the registered EM measurement errors are given by:

$$C_{err} = \sum_{i=0}^{n} N_{i,P}(u) p_{s,i} \tag{1}$$

where N is the NURBS function and p is the control points. Now the EM measurement can be modeled as:

$$C_p = C_s + C_{err} = C_s + \sum_{i=0}^{n} N_{i,P}(u) \Delta p_{err} \tag{2}$$

where C_p and C_s are the measured and real positions, whereas Δp_{err} is the deviation in control points. The problem now is to find a set of control points and their deviation from measurement in order to model the error. Assuming that we have enough measurements and a "round truth" for reference, we can compute C_{err} from above equation and find Δp_{err}. Since the distortion is a function of both translation and orientation of the sensors, one approach to finding Δp_{err} is to interpolate different C_{err} from different orientations:

$$C_{err} = \sum_{i=0}^{3} \alpha_i C_{err}^i \ , \ \sum_{i=0}^{3} \alpha_i = 1 \tag{3}$$

where α_i are the weights for each orientation. Figure 4 shows a 3rd order NURBS curve fit to the errors observed in X, Y and Z axes in a sample dataset. It can be seen that NURBS precisely model the error. The NURBS function computed from the above experiment were then used to correct the error in a subsequent experiment in the same environment. The NURBS was able to improve the measurement error mean from 1.92 to 1.70 mm. Although NURBS were able to model the error more accurately, but it still suffers from the drawback of the high dimensionality of the error space, which is difficult resolve if the number of measurements is sparse. When these corrections were applied to another set of measurements in a second environment, the corrected positions were not improved when compared to ground truth. We believe that no matter how accurately error is modeled, it is not possible to use a single unwarping function to correct for errors in all environments. These methods are time-consuming and can only compensate for static errors in a single environment when the number of calibration sample points is sufficiently large.

2.3 "Absolute" Error Analysis

Error mapping in dynamic environments is the best way of analyzing the workspace of an interventional tool and examine the behavior of the error. It provides the evaluation of the workspace necessary to guide the tool so that tracking and manipulation is kept within interventional zones within which the error is minimal. The experiments in this section were performed to study the change in the "absolute" error map (or errors in the tracking coordinate system) in presence of distortion. Several datasets were collected in an environment which was free of electromagnetic distortion. Then, a small distorter, e.g. metallic components, and a larger distorter, e.g. a magnetic device, were placed in the vicinity of the field generator, close to the interventional field of operation. The error map for a $15 \times 15 \times 15$cm EM tracker measurement volume is shown in Figure 6 for three different environments. In this workspace, the EM field generator is parallel to the Z axis facing the YZ plane (as shown in Figure 5). Comparing these error maps, we observe that the small distorter did not change the error magnitude within the volume whereas the large distorter has increased the error by a factor of three. The accuracy of the system falls off significantly at the edges of the workspace, reflecting the fact that increasing the workspace of the EM tracking system has a significant effect on the accuracy of the system. Interventions need to be constrained within a smaller volume corresponding to a sweet-spot in tracking accuracy.

Figure 7 shows the error map in a $30 \times 30 \times 30$cm cube measured in a "clean" environment and then in the presence of an interventional X-ray scanner (Philips Allura FD20 system, Philips Healthcare). The effects

Downloaded From: http://proceedings.spiedigitallibrary.org/ on 05/10/2013 Terms of Use: http://spiedl.org/terms

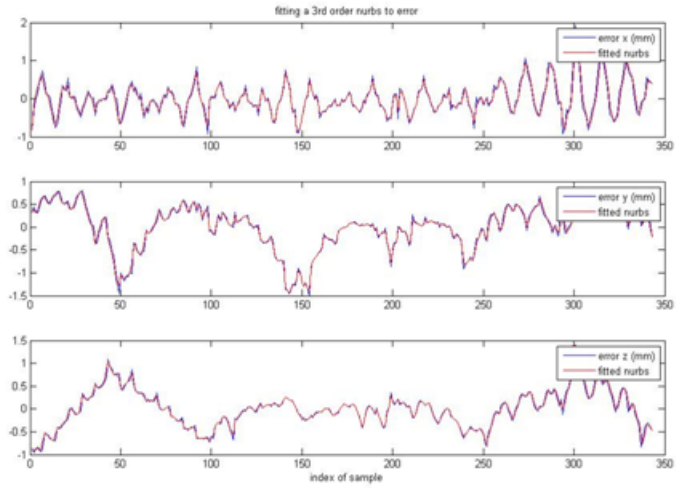

Figure 4. Fitting a 3rd order NURBS to error.

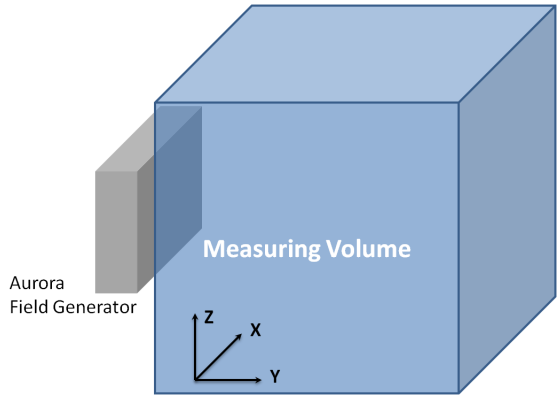

Figure 5. The measuring volume of the Aurora field generator

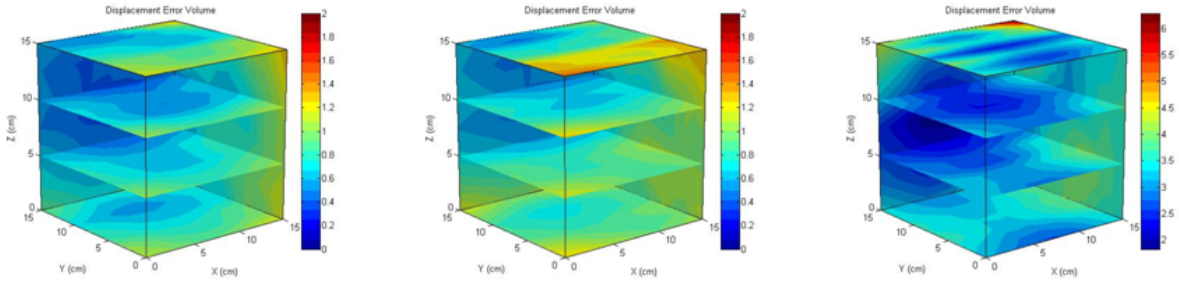

(a) (b) (c)

Figure 6. Error map in a 15x15x15cm workspace of an EM tracker in (a) a "clean" environment, (b) an environment with a small distorter present, and (c) an environment with a big distorter present.

Downloaded From: http://proceedings.spiedigitallibrary.org/ on 05/10/2013 Terms of Use: http://spiedl.org/terms

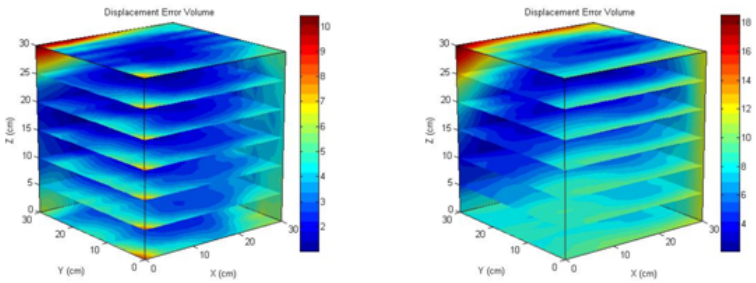

(a) (b) (c)

Figure 7. Error map in a 30x30x30cm workspace of EM tracker in (a) a "clean" environment (b) an interventional X-ray environment.

of large detector/gantry distorer are mainly visible on the edges of the measuring volume. In the center of the tracking volume, the error remains within the reported tolerance of the manufacturer, but clearly the performance diminished in the presence of the X-ray system. The mean of error measured in the interventional scanner environment is 6.53mm. In contrast, within the "clean" environment, the mean error were 3.01mm.

2.4 "Relative" Error

Conventionally, electromagnetic tracking error is defined as the registration error between the EM tracker measurement and a reference navigation system, such as a robot or an optical tracking system. This error is used to determine an error mapping and analyze the workspace of a tool to examine the behavior of the error. It provides an evaluation of the workspace that is necessary to guide manipulation of an interventional instrument within operationing zones for which tracking errors are as small as possible. The mapping of "absolute" errors in dynamic environments is the best way of analyzing the workspace; however, it requires a reference for the tracking system which is not practical in clinical applications. Here, we introduce the concept of "relative" error to estimate the fidelity of the working EM space. We define this error as the difference between the absolute errors in two sensors located at a fixed and known geometry relative to one another. In this approach, error is computed for a reference point in time and space. Subsequent measurement errors are displayed relative to the reference sample point in time to characterize the accuracy in near-real-time. The reference point can be any point in the workspace but usually it is picked within the area with minimum error. The concept of relative error is shown intuitively in Figure 8. The real (known) position of a sensors differs from its tracked position by "absolute" error at each sensor. While the absolute errors might be high, the relative error between the two sensor positions is smaller in magnitude because the error fields measured by each sensor are correlated and fairly homogenous for smoothly-varying spatial distortion field.

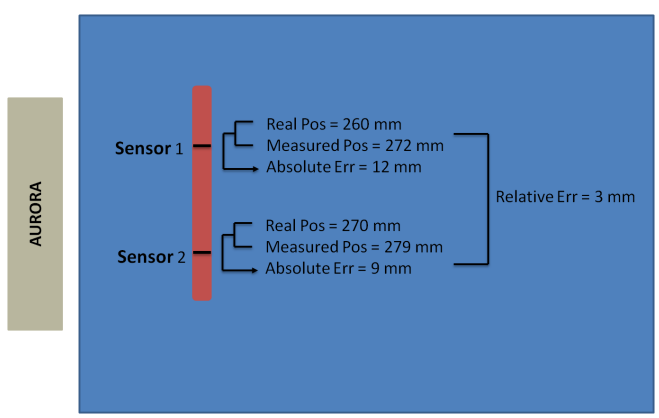

Figure 8. The concept of relative error: relative error is locally homogenous

Downloaded From: http://proceedings.spiedigitallibrary.org/ on 05/10/2013 Terms of Use: http://spiedl.org/terms

2.5 Confidence and Operative Zones

During the phantom calibration step, one can calculate the standard deviation of the error. Since these data are collected in a clean environment, the standard deviation of the error does not reflect any distortion effects. This standard deviation could serve as a baseline for confidence measurement of the error. We define the confidence zone as a sphere centered around the measurement location and with a radius of one error standard deviation. We can define an error confidence metric as:

$$err = std. \parallel R \times N \parallel \tag{4}$$

where R is the nominal unit orientation vector, N is the measured orientation vector, and std is the calculated standard deviation. This sphere is important in the sense that it shows in a non-distorted environment, how much error one should expect in order to make measurements with confidence. In a distorted environment, the relative error is measured and checked to determine if it falls inside the same confidence zone.

In the measurement phase, the position and orientation data from all sensors are compared with the known geometry of the sensor spacing, and localization errors (displacement and orientation) are computed. Based on error thresholds provided by the operator, the spatial distribution of localization errors are clustered and dynamically displayed as separate confidence zones within the operating region of the EM tracker space. Intraprocedural error characterization and visual feedback in this manner can be used to alter interventional paths and/or to reposition medical instrumentation for optimal navigation accuracy.

The thresholding parameter used to assess error characteristics is an important variable in clustering the operative region of the EM tracker space. This parameter determines the different "go / no-go" zones within which the instrument can be operated with clinical confidence. These "go / no-go" zones can be display in near-real-time for visual feedback to the interventionalist and help the clinician correct the trajectory of the instrument to ensure accurate treatment delivery. Visual assessment of the confidence zone allows for immediate feedback that instrument tracking has resulted in a measurement error exceeding a clinically-acceptable threshold magnitude. A more detailed clustering of the operating region is also possible when more than one threshold is given. For example a error transition boundary region, can be visualized when two threshold values are given: one lower threshold corresponding to a green "go" zone, a higher threshold defining a red "no-go" zone, and an orange transition zone between them.

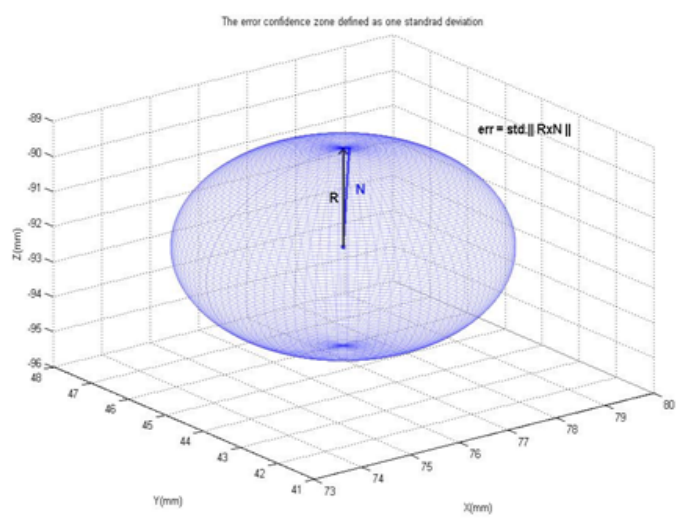

Figure 9. The error confidence zone defined as one standard deviation.

Downloaded From: http://proceedings.spiedigitallibrary.org/ on 05/10/2013 Terms of Use: http://spiedl.org/terms

3. CONCLUSION

A survey of previous error compensation methods demonstrates how these methods are not capable of compensating for errors in dynamic environments. In general, in these methods a set of EM measurement data is registered to a set of reference data and the registration error is modeled with an interpolation function, such as a low-order polynomial basis function. The resulting calibration is applied to distorted EM data to compensate for any measurement errors. These calibration functions are not necessarily valid for as wide a set of measurement conditions as would be desirable for live tracking during interventions. This means that a set of calibration parameters are only applicable for the same static environment that they are predicated in. These parameters cannot be carried over to other environments, requiring recalibrating as the environment changes over time. .

Studying the behavior of the NDI Aurora EM tracking system in a distorted environment revealed that measurements in a 10x10x10cm cube in the center of EM field generator show acceptable measurement errors of less than 1 mm. When this volume is increased to a 15x15x15cm the error increased to a maximum of 2mm but these errors were still in a range that satisfies the requirements of most tracking applications. In a 30x30x30cm workspace, the tracking error could be as high as 10mm, which clearly is not acceptable. Selecting the operational workspace of the EM tracking is essential to ensuring usable measurement results.

The effects of different types of the EM distortion were studied on EM tracking accuracy. It was seen that a small distortion, such as introduced by pieces of metal around the field generator and a metal bar 2-3cm away from sensor coils, has negligible impact on measurement quality. On the other hand, a large distorter, such as a power supply placed in close proximity to the field generator or a large metallic structure placed close to the field generator, produced significant measurement errors.

The concept of "relative" error was introduced and it was shown that this error is locally homogenous. When compared to "absolute" error, "relative" error provides a much larger workspace and is associated with smaller error magnitudes. Since relative error is easy to compute in real time, it could provide immediate information about measurement confidence or reliability of localization estimates. A go/no go approach was presented that determines on the usability of measurement based on a comparison of relative error and a user defined threshold. When the computed relative error is less than a specified threshold, the measurement is deemed acceptable, presenting a "go" measurement. In contrast, when the error exceeds the threshold, the measurement location is deemed a "no-go" point, requiring adjusting of the treatment approach. We discussed the use of the error standard deviation of measurement obtained during phantom calibration in a "clean" environment as a gating metric for visual assessment of the confidence zone in real-time measurements. For each measurement, the zone with a radius less than calibration standard deviation is a zone with reliable estimates. In combination, the intra-procedural error characterization and visual feedback approach described here can be used to alter interventional paths and/or to re-position medical instrumentation for optimal navigation accuracy.

REFERENCES

[1] Nafis, C., Jensen, V., and Jako, R. V., "Method for evaluating compatibility of commercial electromagnetic (em) microsensor tracking systems with surgical and imaging tables," in [*Medical Imaging: Visualization, Image-guided Procedures, and Modeling*], *Proc. SPIE* **9618**, 691–820 (2008).

[2] Shen, E., Shechter, G., Kruecker, J., and Stanton, D., "Effects of sensor orientation on ac electromagnetic tracking system accuracy in a ct scanner environment," in [*Medical Imaging: Visualization, Image-guided Procedures, and Modeling*], *Proc. SPIE* **9618**, 11–23 (2008).

[3] Kindratenko, V., "A survey of electromagnetic position tracker calibration techniques," *J. Virtual Reality* **5**, 169–182 (2000).

[4] Wilson, E., Yaniv, Z., Zhang, H., Nafis, C., Shen, E., Shechter, G., Wiles, A., Peters, T., Lindisch, D., and Cleary, K., "A hardware and software protocol for the evaluation of electromagnetic tracker accuracy in the clinical environment: a multi-center study," in [*Medical Imaging: Visualization, Image-guided Procedures, and Modeling*], *Proc. SPIE* **6509**, 65092T1–65092T11 (2007).

[5] Frantz, D., Wiles, A., Leis, S., and Kirsch, S., "Accuracy assessment protocols for electromagnetic tracking systems," *J. Physics in Medicine and Biology* **48**, 2241–2251 (2003).

Downloaded From: http://proceedings.spiedigitallibrary.org/ on 05/10/2013 Terms of Use: http://spiedl.org/terms

[6] Fischer, G. S. and Taylor, R., "Electromagnetic tracker measurement error simulation and tool design," in [*Medical Image Computing and Computer-Assisted Intervention*], *Proc. MICCAI*, 73–80 (2005).

[7] Fischer, G. S., [*Electromagnetic Tracker Characterization and Optimal Tool design with Application to ENT Surgery*], Johns Hopkins University, M.Sc. Thesis (2005).

[8] Piegl, L., "On NURBS: A survey," *IEEE Computer Graphics and Applications* **11**, 55–71 (1991).

Downloaded From: http://proceedings.spiedigitallibrary.org/ on 05/10/2013 Terms of Use: http://spiedl.org/terms